Supporting Information

Chemical Composition-Dependent Hygroscopic Behavior of Individual Ambient Aerosol Particles Collected at a Coastal Site

Li Wu[1,2,+], Hyo-Jin Eom[1,3,+], Hanjin Yoo[1,4], Dhrubajyoti Gupta[1], Hye-Rin Cho[1], Pingqing Fu[2], and Chul-Un Ro[1,4,*]

[1] Department of Chemistry, Inha University, Incheon 22212, Korea

[2] Institute of Surface-Earth System Science, School of Earth System Science, Tianjin University, Tianjin 300072, China

[3] Air Quality Research Division, National Institute of Environmental Research, Incheon 22689, Korea

[4] Particle Pollution Management Center, Inha University, Incheon, 21999, Korea

[*] *Correspondence to* Chul-Un Ro (curo@inha.ac.kr)

[+] Authors with equal contributions

Table S1. Elemental concentrations (in at.%) of 37 ambient particles determined by low-*Z* particle EPMA (SSAs #15 and #27 are not included here due to the recombination of the particle after hygroscopic process).

Particle group	Mole fractions $X_{(Na,\,Mg)Cl}$	No.	Size (µm)	C	N	O	Na	Mg	Al	Si	S	Cl	K	Ca	Cr	Mn	Fe
SSAs Cl-rich	0.75	5	4.93	29.7	4.3	17.5	22.1	2.8			1.4	20.9	0.6	0.7			
	0.76	3	3.81	36.4	4.4	19.0	19.5	1.6			0.9	17.3	0.5	0.4			
	0.76	24	4.97	24.7	7.3	18.6	24.0	2.0			1.1	21.2	0.5	0.6			
	0.71	19	4.43	35.5	5.9	17.0	20.3	2.2			0.9	17.6	0.4	0.3			
	0.68	21	4.26	38.3	6.5	19.4	17.6	1.9			1.0	14.5	0.4	0.4			
	0.65	13	4.76	34.6	8.3	18.3	19.5	2.0			1.1	15.2	0.4	0.5			
	0.61	9	3.73	46.1	6.1	21.4	13.3	1.6			0.7	10.1	0.3	0.3			
	0.55	26	3.80	49.3	4.6	23.3	11.9	1.4			0.9	8.1	0.2	0.3			
	0.52	23	4.56	47.4	6.0	23.0	12.3	1.6			0.9	8.0	0.4	0.3			
	0.41	35	3.84	48.0	8.2	25.7	10.4	1.3			0.7	5.3	0.2	0.2			
SSAs Cl-depleted	0.34	1	4.64	44.8	11.0	24.9	11.6	1.5			0.8	4.9	0.2	0.2			
	0.29	31	3.36	49.3	7.5	25.0	11.2	1.5			1.0	4.1	0.2	0.3			
	0.28	33	5.27	46.3	8.0	27.9	11.3	1.4			0.7	4.0	0.2	0.2			
	0.29	22	4.82	50.0	8.1	26.2	9.8	1.2			0.5	3.5	0.3	0.3			
	0.27	39	4.88	45.7	10.2	28.1	10.1	1.2			0.7	3.4	0.3	0.3			
	0.25	30	4.33	47.8	8.4	30.0	8.9	1.1			0.6	2.8	0.2	0.2			
	0.25	10	3.65	50.2	8.6	27.0	9.4	1.0			0.5	2.8	0.2	0.3			
	0.23	11	2.94	50.6	8.3	26.3	9.8	1.2			0.5	2.8	0.3	0.3			
	0.22	12	2.70	43.6	6.7	33.8	10.6	1.2			0.9	2.9	0.2				
	0.15	16	3.79	38.4	12.8	32.7	11.1	1.2			1.0	2.1	0.3	0.2			
	0.15	6	4.12	43.4	9.8	29.6	11.9	1.6			0.8	2.3	0.2	0.3			
	0.15	18	3.17	46.9	12.5	26.0	12.6				0.1	1.9					
	overall average			43.0	7.9	24.6	13.6	1.5			0.8	8.0	0.3	0.3			
	standard deviation			7.2	2.3	4.9	4.6	0.4			0.3	6.6	0.1	0.1			
Ca-containing		17	3.01	23.2	8.0	50.7		2.6	1.7	5.1		0.6	0.3	7.8			
		20	3.87	20.7	7.4	49.7		0.4	0.2	0.2		0.7		20.6			
		25	5.84	33.5	4.3	48.5		4.8	0.2	0.3	0.1	0.2		8.2			
		34	2.47	19.8	5.6	56.4		0.4	2.1	4.0		0.1		10.8			0.9
		38	3.64	20.9	8.7	50.4		0.5	0.4	0.3	3.7	1.1		14.0			
Alumino-silicates		4	1.87	23.4		49.5		1.1	7.4	12.6	0.2	0.2	1.1	0.6		1.6	2.2
	aged	8	3.35	22.8	7.0	48.7		1.1	4.1	8.5		0.3	0.5	5.5			1.4
	aged	14	2.98	13.4	3.6	48.6	4.8	5.0	5.0	12.0	0.7	0.7	1.0	3.4			1.9
	aged	28	2.89	14.1	3.8	50.0	0.9	5.2	6.1	12.8	0.4	0.2	1.8	3.2			1.4
		29	2.35	1.5		57.7	6.2		8.7	25.9							
		32	2.38	17.6		44.0		1.4	9.4	19.5			1.1	0.6		2.8	3.7
SiO$_2$	aged	37	2.05	9.2	2.9	59.5		0.8	3.1	22.4			0.8	0.9			0.5
Organic and ammonium sulfate		36	2.21	75.1	4.1	10.2					10.7						
Fe-rich		2	1.93	24.7		39.7				0.5		1.1			3.0		31.0
		7	2.50	22.1	0.0	18.7			0.6	11.6					7.2		39.9

Figure S1. Optical images of the second field (particles #17 - #26) during humidifying (A-F, ↑) and dehydration (G-K, ↓) processes and the SEI of the same field (L).
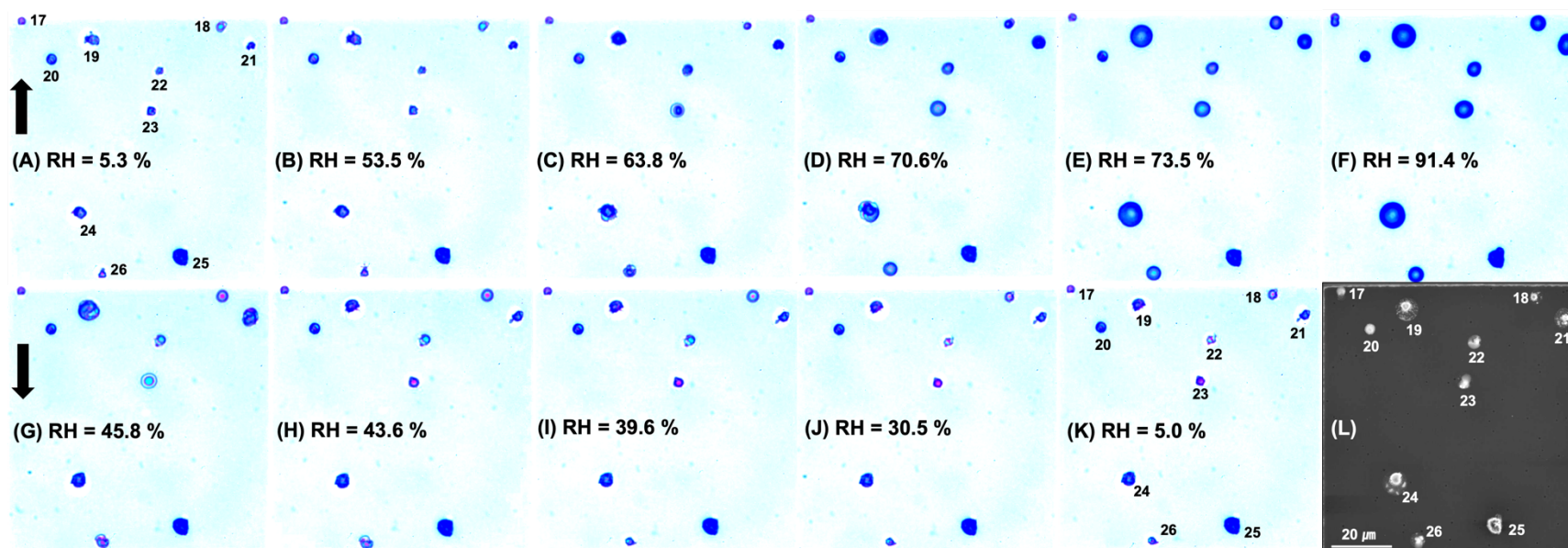
Figure S2. Optical images of the third field (particles #27 - #39) during humidifying (A-F, ↑) and dehydration (G-K, ↓) processes and the SEI of the same field (L).
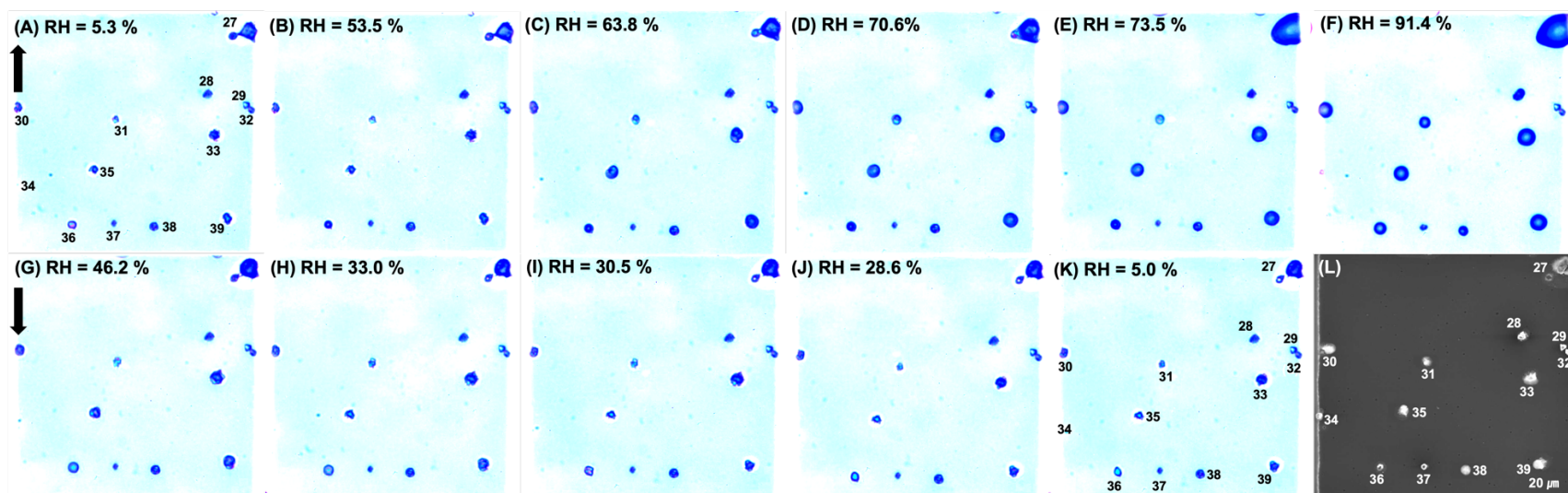
Figure S3. 2-D area ratio plots of (Na, Mg)(Cl, NO₃) aerosols as a function of RH.
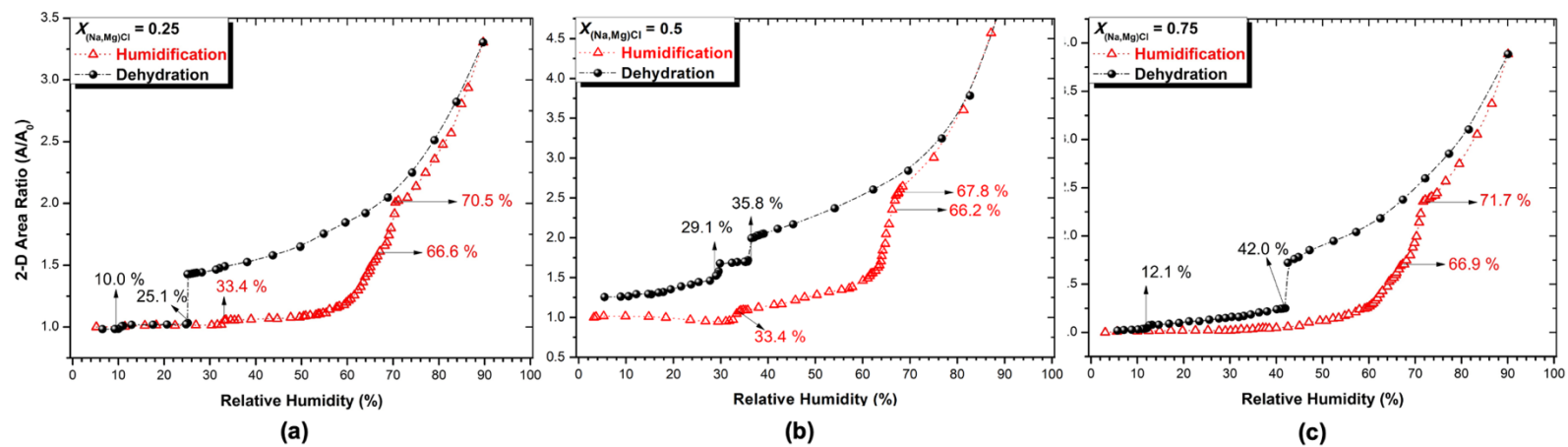
Figure S4. X-Ray elemental maps for C, N, O, Na, Mg, S, Cl, and Ca and secondary electron images (SEIs) of the effloresced ambient SSAs: (a) SSA #5 and (b) SSA #19 with Cl-rich compositions of $X_{(Na,Mg)Cl}$ = 0.75 and 0.72, respectively.
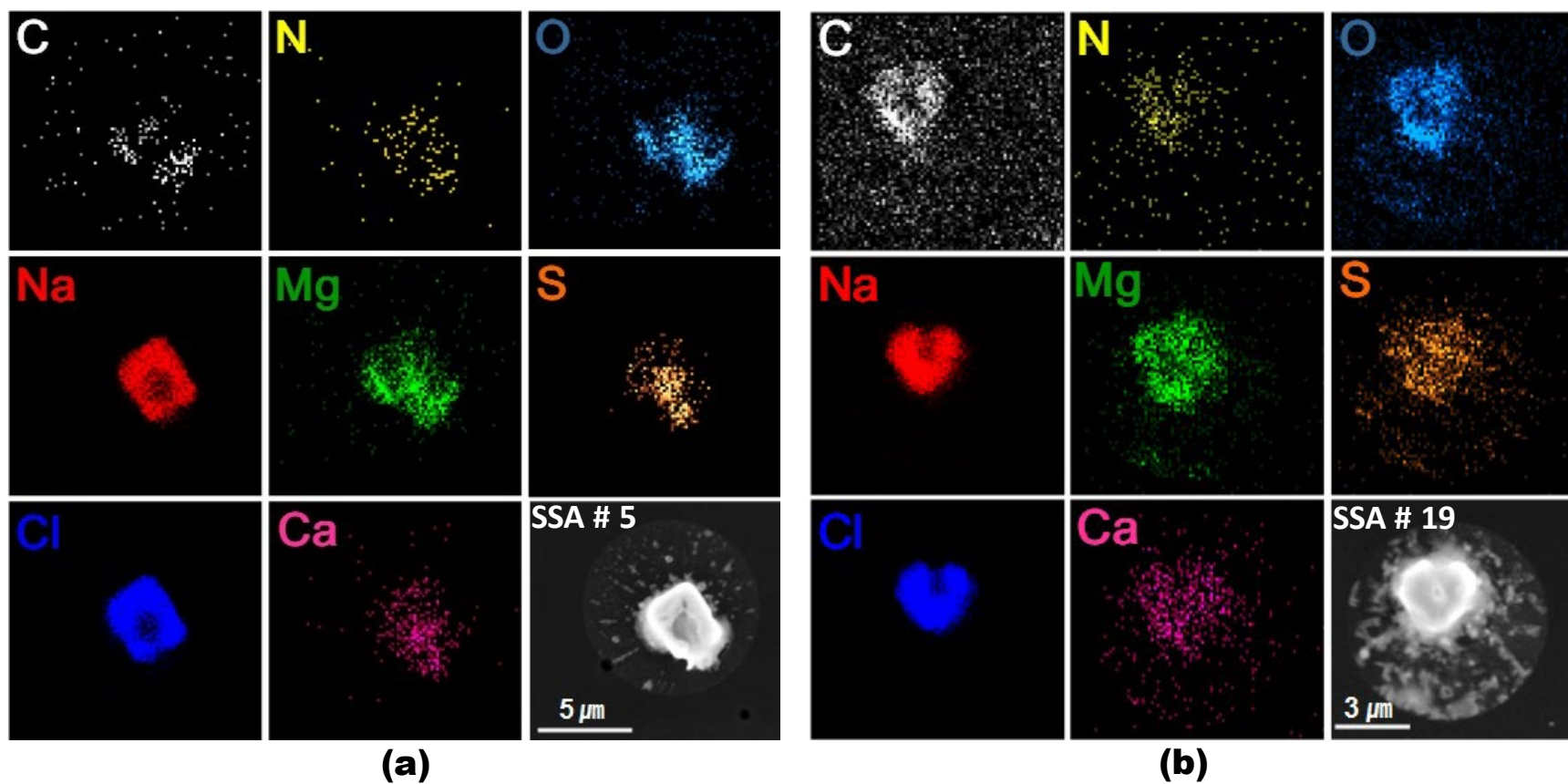
Figure S5. X-Ray elemental maps for C, N, O, Na, Mg, S, Cl, and Ca and secondary electron images (SEIs) of the effloresced ambient SSAs: (a) SSA #23 and (b) SSA #11 with equimolar and Cl-depleted compositions of $X_{(Na,Mg)Cl}$ = 0.52 and 0.23, respectively.
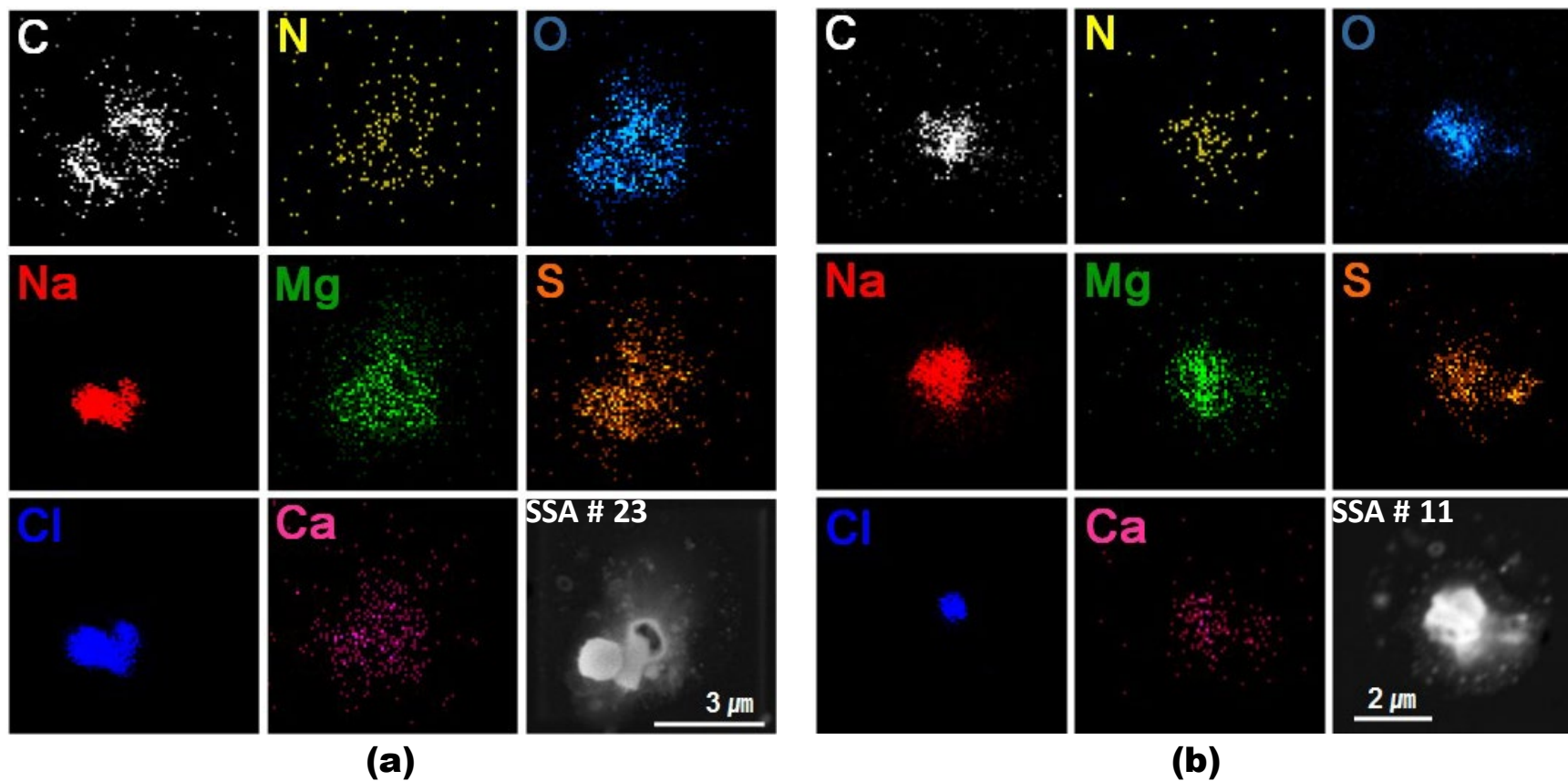
Figure S6. 2-D area ratio plot and X-ray spectrum of an aged aluminosilicate particle mixed with SSA (particle #14)
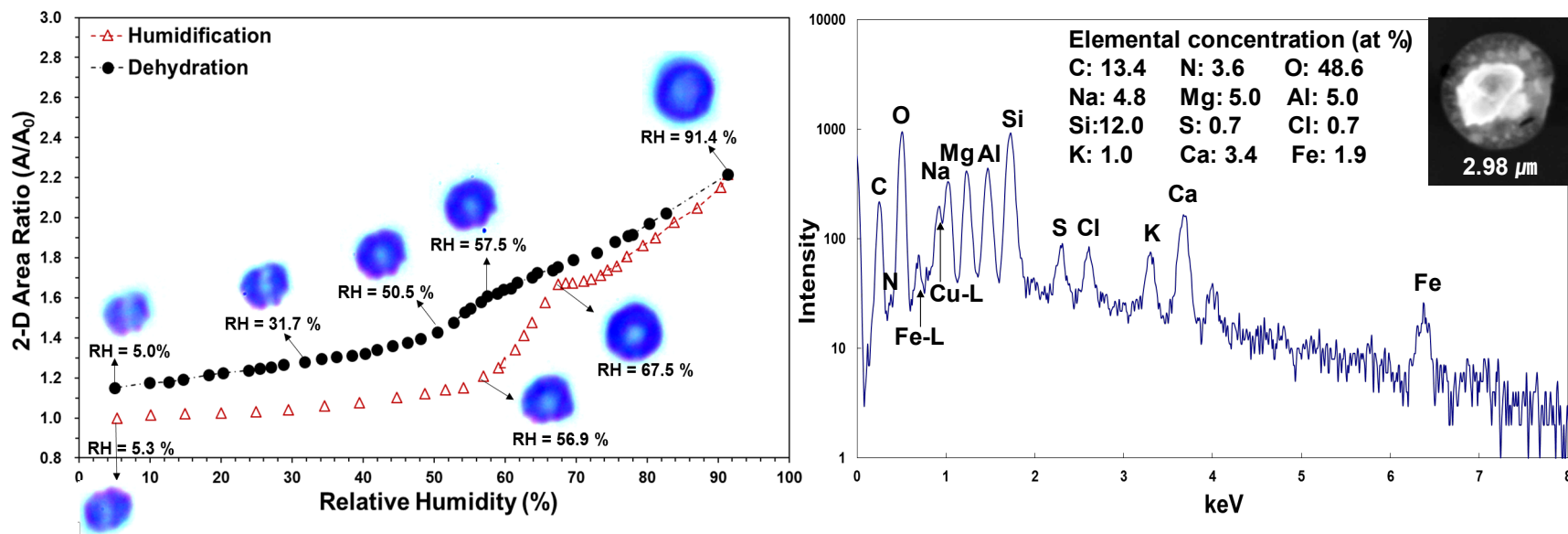
Figure S7. 2-D area ratio plot and X-ray spectrum of a reacted Ca-containing particle (particle #20).
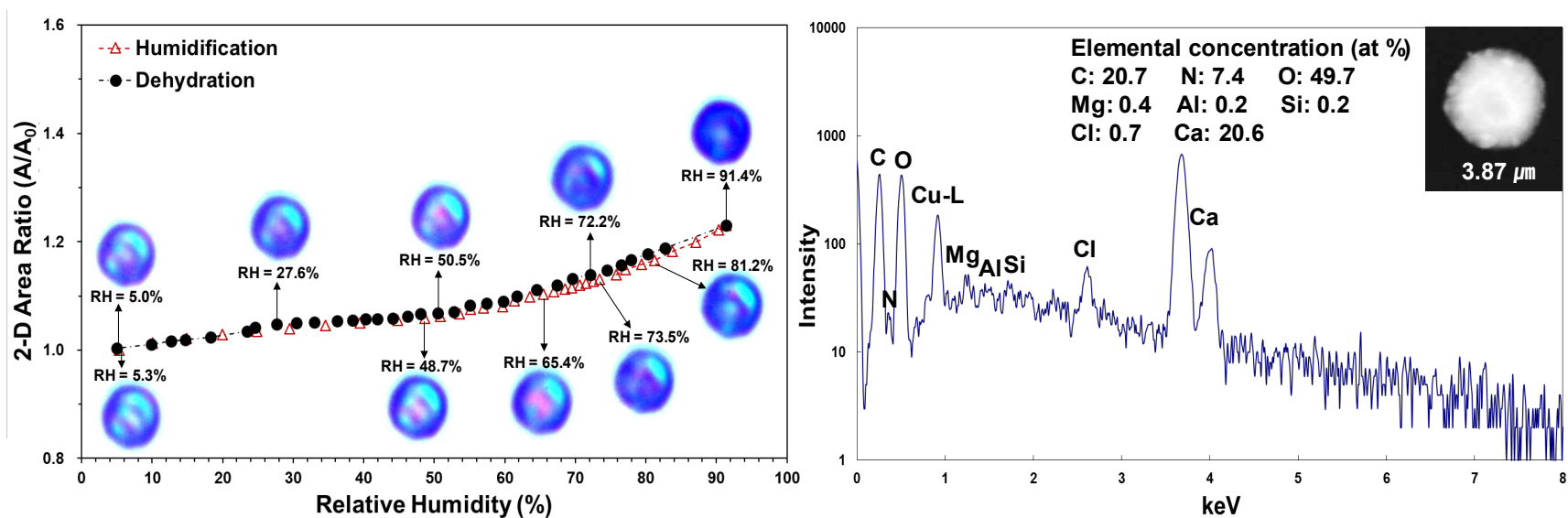
Figure S8. 2-D area ratio plot and X-ray spectrum of an ammonium sulfate aerosol mixed with organics (particle #36).
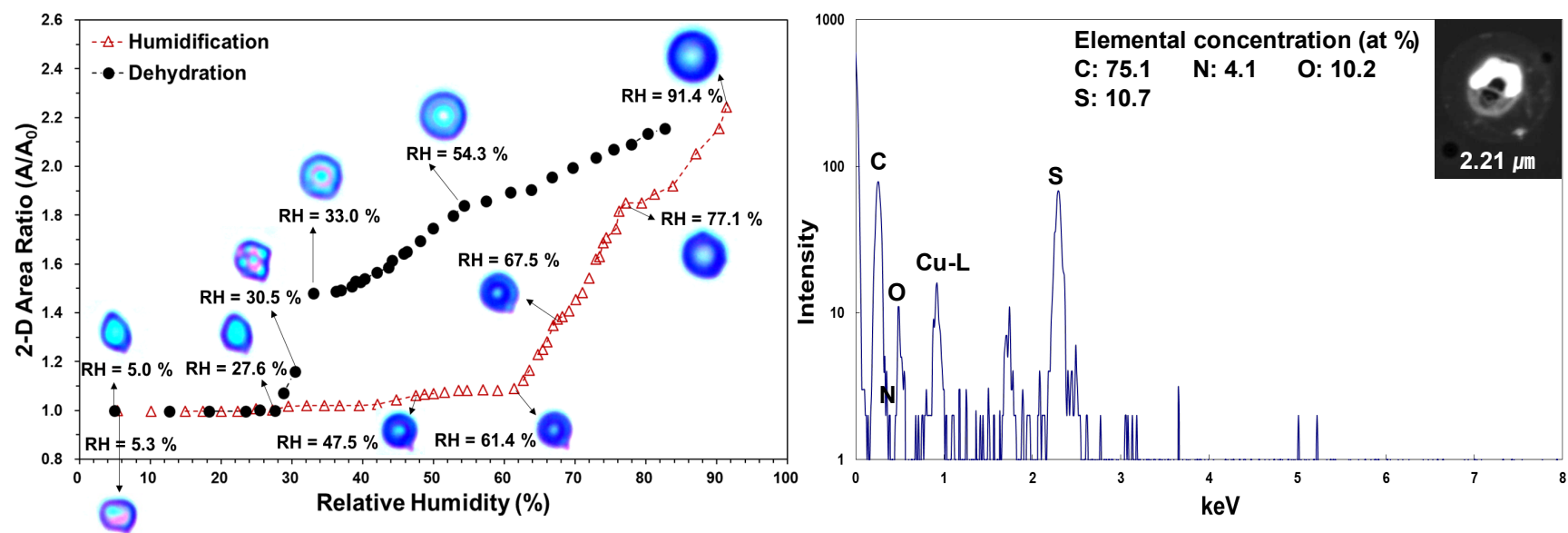
Figure S9. 2-D area ratio plots and X-ray spectra of partially reacted Ca-containing particles (particles #17 and #25).
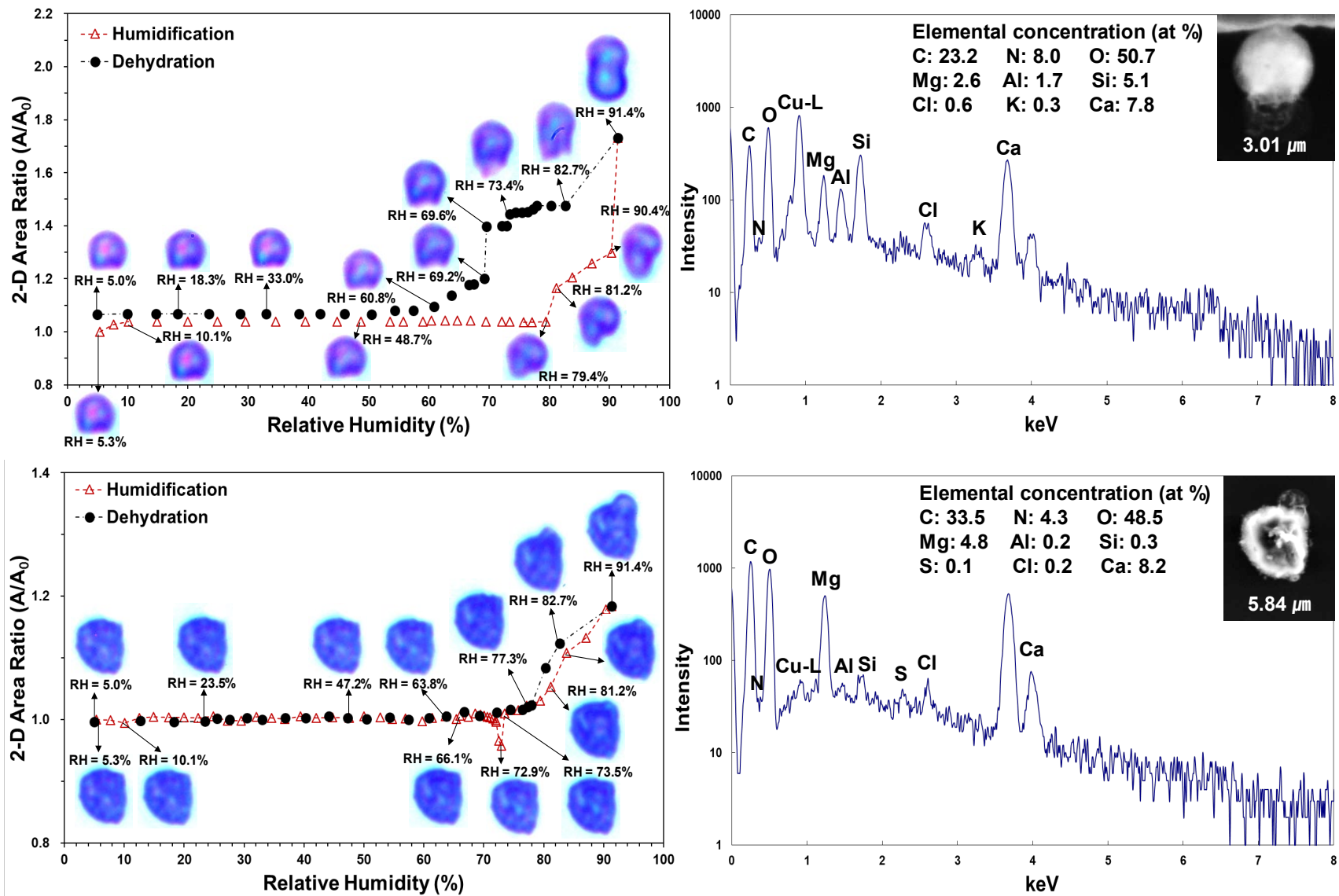
Figure S10. 2-D area ratio plot and X-ray spectrum of partially aged SiO$_2$ particle (particle #37).
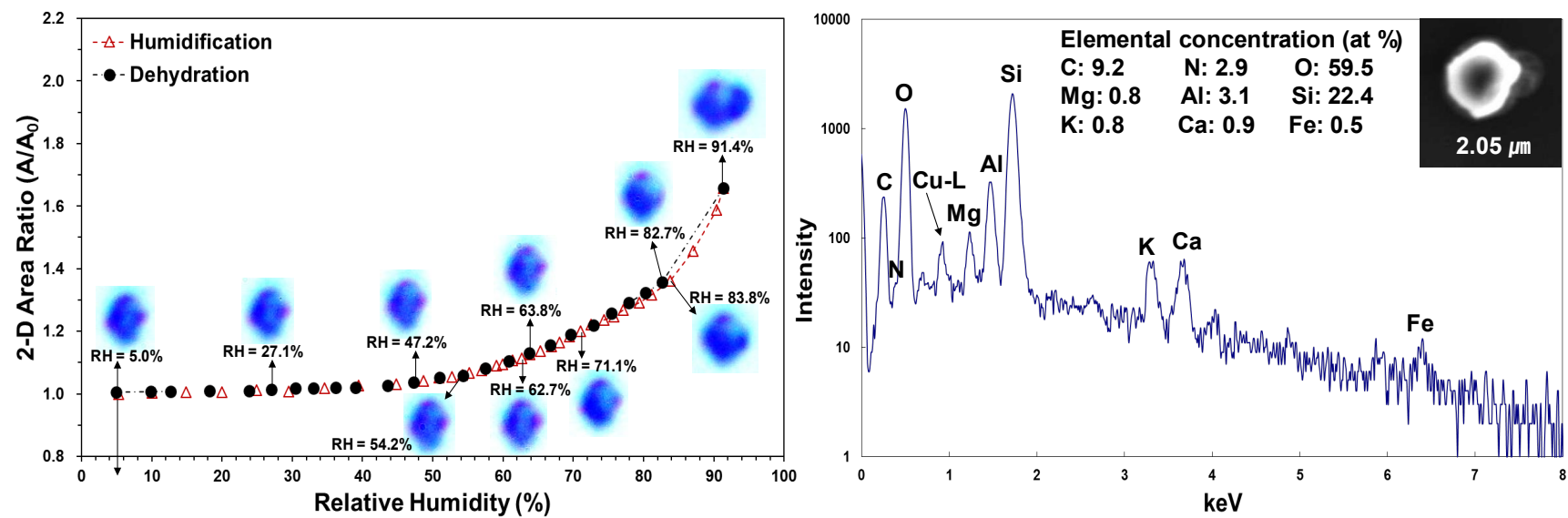
Figure S11. 2-D area ratio plots and X-ray spectra of aluminosilicate particles (particles #29 and #32).
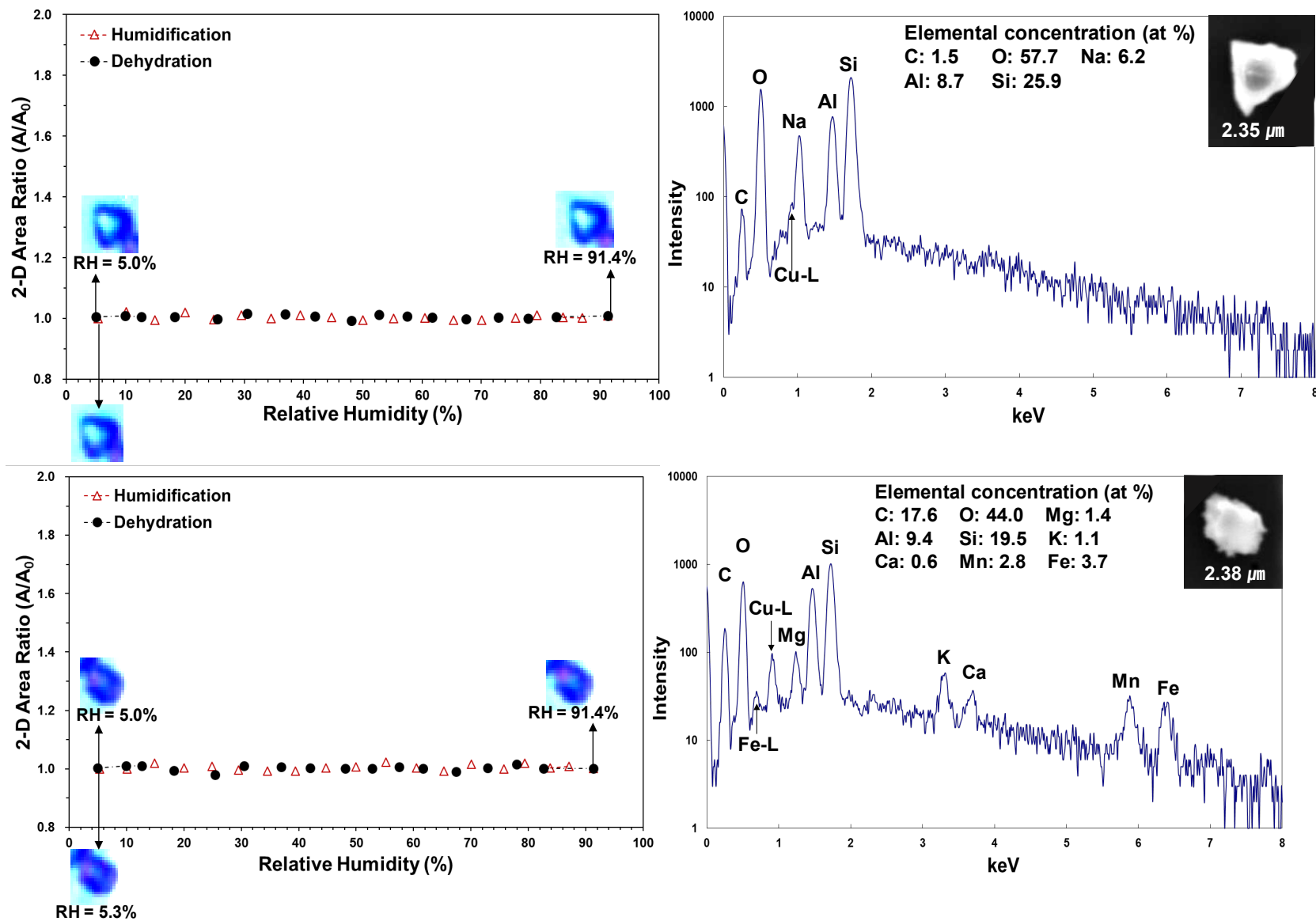
Figure S12. 2-D area ratio plots and X-ray spectra of Fe-rich particles (particles #2 and #7).